

Probing Carbon Nanotube–Surfactant Interactions with Two-Dimensional DOSY NMR

Tejas A. Shastry,[†] Adam J. Morris-Cohen,[‡] Emily A. Weiss,^{*,‡} and Mark C. Hersam^{*,†,‡}

[†]Department of Materials Science and Engineering and [‡]Department of Chemistry, Northwestern University, Evanston, Illinois 60208, United States

Supporting Information

ABSTRACT: Two-dimensional diffusion ordered spectroscopy (2D DOSY) NMR was used to probe the micellar structure of sodium dodecyl sulfate (SDS) and sodium cholate (SC) in aqueous solutions with and without semiconducting and metallic single-walled carbon nanotubes (SWCNTs). The solutions contain SDS and SC at weight ratios of 1:4 and 3:2, the ratios commonly used to isolate semiconducting and metallic SWCNTs through density gradient ultracentrifugation (DGU). These results show that the coverage of surfactant on the semiconducting and metallic SWCNTs is nearly identical in the 1:4 surfactant mixture, and a lower degree of bundling is responsible for the greater buoyancy of semiconducting SWCNTs. In the 3:2 surfactant mixture, the metallic SWCNTs are only encapsulated in SC while the semiconducting SWCNTs remain encapsulated in a poorly packed two-surfactant micelle, leading to a large buoyant density difference between the electronic species. This work provides insight into future directions to increase the purity of semiconducting and metallic SWCNTs sorted through DGU and demonstrates the utility of 2D DOSY NMR in probing SWCNT–surfactant complexes.

Density gradient ultracentrifugation (DGU) separates polydisperse mixtures of single-walled carbon nanotubes (SWCNTs) by their electronic type,¹ chirality,² diameter,³ and handedness,⁴ enabling the exploration of a variety electronic⁵ and optoelectronic⁶ applications involving homogeneous SWCNT solutions. DGU separation is enabled by subtle buoyant density differences between complexes formed by different types of SWCNTs and their encapsulating surfactants.¹ One of the most common DGU separations involves isolating metallic or semiconducting SWCNTs from an electronically polydisperse mixture using a combination of two anionic surfactants—sodium cholate (SC) and sodium dodecyl sulfate (SDS).¹ Despite widespread use of this technique, the mechanism by which these surfactants interact with the two types of SWCNTs to produce buoyant density differences is largely unknown. The primary difference between semiconducting and metallic SWCNTs is that metallic SWCNTs are more polarizable; this difference in polarizability is thought to play a key role in determining the SWCNT–surfactant structure.¹

In this Communication, we utilize two-dimensional diffusion-ordered spectroscopy (2D DOSY) NMR to probe the micellar structure of aqueous co-surfactant systems comprising SDS and

SC at the two surfactant ratios under which DGU produces metallic and semiconducting enriched SWCNT dispersions. The DOSY NMR spectra reveal the size of the micelles formed in the co-surfactant systems and the perturbations to the micellar structures in the presence of metallic and semiconducting SWCNTs. These experiments shed light on the contribution of different micellar structures in producing buoyant density differences between metallic and semiconducting SWCNTs and suggest a mechanism by which these differences arise.

Efforts to elucidate the origins of electronic-type DGU sorting have focused on studying and modeling the interaction of SWCNTs and individual surfactants. Molecular dynamics simulations find similar binding energies for SC and SDS on the surface of different types of SWCNTs, confounding explanations for the large buoyant density differences observed.⁷ Analytical ultracentrifugation has proven useful in determining the packing density of a single surfactant on a single SWCNT species, revealing the importance of a local hydration layer around the SWCNT–surfactant complex in determining the precise density. However, these experiments, and other centrifugation studies,⁹ are limited to single-surfactant systems and cannot simultaneously probe interactions between two ionic surfactants and SWCNTs to explain buoyant density differences in the complex environments that are critical for electronic-type separations.⁸ Previously, NMR spectroscopy and 2D DOSY NMR have been used to probe the interactions between molecules and nanostructures,¹⁰ including SWCNTs.^{11,12} By decomposing the NMR spectrum of a dispersion along the diffusion dimension, changes in *D* for various components can be identified and correlated to changes in interaction with other components. 2D DOSY NMR therefore offers a platform to probe multi-component systems, such as aqueous solutions of surfactant-encapsulated SWCNTs.

To study the effect of SWCNT electronic type on surfactant micellar structure (and therefore buoyant density), we prepared highly enriched samples of metallic and semiconducting SWCNTs with similar surface area through a previously described dual-iteration DGU strategy.³ The first DGU iteration narrows the diameter distribution of the SWCNTs, while the second DGU iteration sorts the diameter-enriched fractions by electronic type. Isolation of metallic and semiconducting species of nearly identical diameter and length distribution ensures that observed differences in the diffusion of SWCNT–surfactant complexes are due to differences in the SWCNT electronic type,

Received: December 14, 2012

Published: February 1, 2013

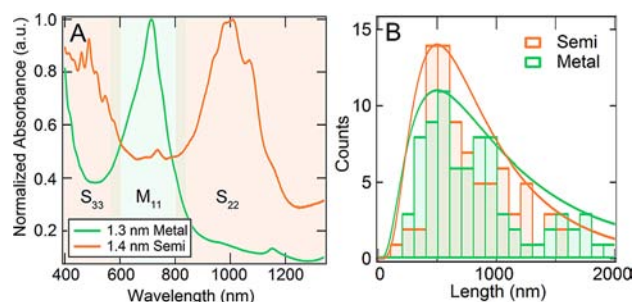


Figure 1. (A) Ground-state optical absorption spectra of metallic and semiconducting SWCNTs with purities greater than 98% and diameters of 1.3 ± 0.1 and 1.4 ± 0.1 nm, respectively. (B) Length distributions of semiconducting and metallic SWCNTs with peak values at 500 nm.

not differences in the average size of the SWCNTs. Figure 1A shows the ground-state absorption spectra of the metallic and semiconducting SWCNTs, where suppression of the M11 and S22 peaks in the semiconducting and metallic samples, respectively, indicates electronic-type enrichment greater than 98%. Through analysis of the radial breathing mode from Raman spectroscopy and the ground-state absorption spectra, we determined the diameters of the metallic and semiconducting SWCNTs to be 1.3 ± 0.1 and 1.4 ± 0.1 nm, respectively. The length distributions of the electronic-type enriched samples in Figure 1B are also well matched and fit a log-normal distribution with a peak length of 500 nm. The similarities in diameter and length distribution indicate comparable surface area in the SWCNT samples; i.e., the principal difference between the SWCNT samples is the electronic type. The Supporting Information (SI) contains details of the DGU procedure and the characterization of SWCNT length and diameter.

Figure 2 shows 2D DOSY NMR spectra for 1% (w/v) surfactant solutions of SDS and SC at weight ratios of 1:4 and 3:2 in deuterated water (see SI for details). These are the co-surfactant ratios used in DGU sorting to isolate semiconducting and metallic SWCNTs, where 1:4 results in semiconducting SWCNTs as most buoyant while 3:2 results in the metallic species as most buoyant. As the critical micelle concentrations (CMCs) of SDS and SC are 0.2% and 0.3–0.6% (w/v), respectively, SDS completely forms micelles in both ratios, while all SC molecules form micelles in the 1:4 sample and only about a third form micelles in the 3:2 sample.¹³ The DOSY data are plotted in the chemical shift and diffusion dimensions; a trace along a specific diffusion constant (D) gives the ^1H spectrum of the species diffusing at that rate. The spectra along the tops of the figures are the integrated sums of signals from all protons at a given chemical shift, and those along the left sides are the integrated sums of signals from all protons at a given D .

The integrated spectrum of all chemical shifts on the left of Figure 2A exhibits two sharp peaks: the top (faster-diffusing) peak corresponds to the ^1H spectrum of SC while the bottom peak corresponds to that of SDS.¹⁴ We verified the identity of the peaks denoted SC and SDS by examining the ^1H spectra in the chemical shift dimension at a given D , and comparing them to 1D ^1H spectra of the individual molecules. These two distinct peaks indicate the presence of two single-surfactant micelles diffusing at different rates in the 1:4 solution, where the Stokes–Einstein relation predicts micelle radii of 0.83 and 1.03 nm for the SC and SDS micelles, respectively, based on the peak D values (see SI for peak identity and radius calculations). Given that the SC micelle is normally smaller than the SDS micelle,¹³ our finding that the

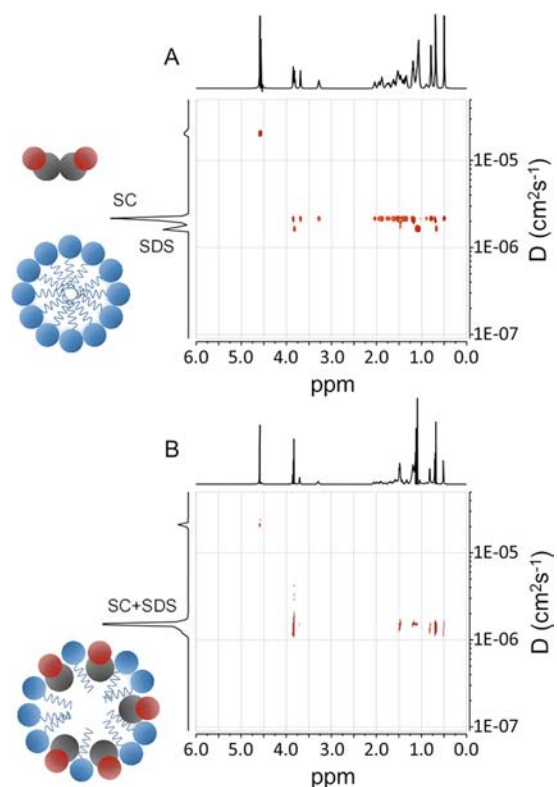


Figure 2. 2D DOSY NMR spectra of (A) 1:4 and (B) 3:2 SDS:SC surfactant only (no SWCNTs) samples. Integration of all chemical shifts (ppm) vs diffusion constant (D) is plotted on the left, while integration of all diffusion constants vs chemical shift is plotted at the top of each graph. Single-surfactant micelles of SC and SDS in 1:4 SDS:SC, and two-surfactant micelle composed of both SDS and SC in 3:2 SDS:SC, are drawn next to the corresponding micelle peak.

SC micelle diffuses faster than the SDS micelle is reasonable. Figure 2B, however, shows a single sharp peak in the integrated diffusion spectrum on the left axis, indicating that the 3:2 solution contains a single mixed micelle comprising both surfactants. This mixed micelle diffuses slower than either of the single-surfactant micelles in the 1:4 mixture, with a predicted radius of 1.15 nm. Other NMR studies of mixed SDS/SC systems also find that at small concentrations of SC, SC molecules enter the SDS micelle rather than form their own micelles.¹⁵ As the concentration of SC in the 3:2 mixture is just above the CMC for SC, these reports are consistent with our observation of mixed micelles. Figure 2 also shows cartoons of the two single-surfactant micelles in the 1:4 SDS:SC mixture, and the mixed micelle in the 3:2 SDS:SC mixture. Both panels in Figure 2 exhibit a small H_2O peak at 4.6 ppm, which arises from H_2O impurities in the deuterated water. As the majority of the density gradient medium, iodixanol, was removed by dialysis before all NMR experiments, we do not observe its presence in any of the NMR data and cannot comment on its role in electronic-type separation.

To study the effect of SWCNTs on the diffusion of SDS and SC, we added various amounts of semiconducting SWCNTs to the 1:4 and 3:2 surfactant solutions. Figure 3 shows traces along the diffusion dimension integrated across all chemical shifts—the same type of traces drawn along the y -axes in Figure 2—for 1:4 and 3:2 SDS:SC mixtures. The four curves show semiconducting SWCNT loadings of 0 (no SWCNTs), 0.01, 0.05, and 0.7 mg/mL, with the identity of the surfactant peaks denoted; the 0 mg/mL traces in Figure 3 are identical to the traces in Figure 2.

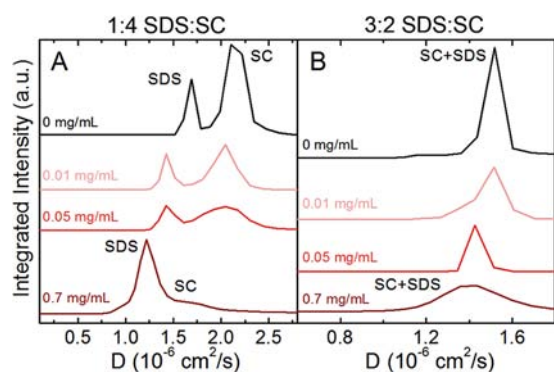


Figure 3. Integrated intensity versus diffusion constant for surfactant-only and semiconducting SWCNT samples with surfactant ratios (A) 1:4 and (B) 3:2 SDS:SC, at various SWCNT concentrations.

Previous studies have determined D for SWCNTs in aqueous solutions to be between 0.3×10^{-10} and $6 \times 10^{-10} \text{ cm}^2 \text{ s}^{-1}$,¹⁶ but we observe no peaks from the surfactants in this range. The lack of peaks at these D values suggests the surfactant molecules are in fast chemical exchange (with respect to the NMR time scale) between the SWCNT micelles and their native micellar state.¹⁷ The relevant NMR time scale in the DOSY experiment is 150 ms, during which the sample is allowed to diffuse. If during that time the surfactant molecules exchange between micelles containing SWCNTs, which diffuse very slowly, and their native micelles, which diffuse at the rate of the micelles in the surfactant-only state, the measured diffusion constant will be a weighted average of the D values of the molecules in these two states. Inspection of the traces for samples containing semiconducting SWCNTs in Figure 3 shows that, for both ratios of SDS to SC, the surfactants diffuse, on average, more slowly in the presence of SWCNTs than without added SWCNTs, as expected for surfactants in fast exchange between the two states. The peaks corresponding to single-surfactant micelles in the 1:4 mixture coalesce with increasing concentration of SWCNTs as a result of the SC peak shifting more than the SDS peak. The SC peak also broadens more than the SDS peak as both surfactants spend increasing time on the SWCNTs. The broad SC peak arises from slow exchange between free micelles and SWCNT-encapsulating micelles, while the sharp SDS peak signifies faster exchange, indicating that a larger fraction of SC adsorbs to the SWCNTs than SDS. These peak characteristics support the hypothesis presented in previous literature that the SC molecules predominately, but not completely, cover the SWCNT surface, and that SDS serves to “plug” the remaining holes.¹ Within the 3:2 mixtures, the mixed-micelle peak also broadens and shifts to a slower D with increasing SWCNT concentration.

In Figure 4, we compare the diffusion of SDS and SC with high concentrations of semiconducting and metallic SWCNTs ($\sim 0.7 \text{ mg/mL}$) at surfactant ratios of 1:4 (Figure 4A) and 3:2 (Figure 4B). In the case of 1:4, both electronic types decrease the average D of both surfactants, but it appears that both surfactants spend slightly more time on the semiconducting SWCNTs than on the metallic SWCNTs (Table S1). The shapes of the SC and SDS peaks are similar in both species: the SDS peak is sharp, and the SC peak is broad. We can conclude from these spectra that the metallic and semiconducting SWCNTs draw very similar surfactant coverage from the single-surfactant micelles present in the 1:4 mixtures (as depicted in the cartoon in Figure 4C).

In the sample with a 3:2 ratio of SDS:SC with semiconducting SWCNTs, the single peak in the DOSY spectrum indicates that

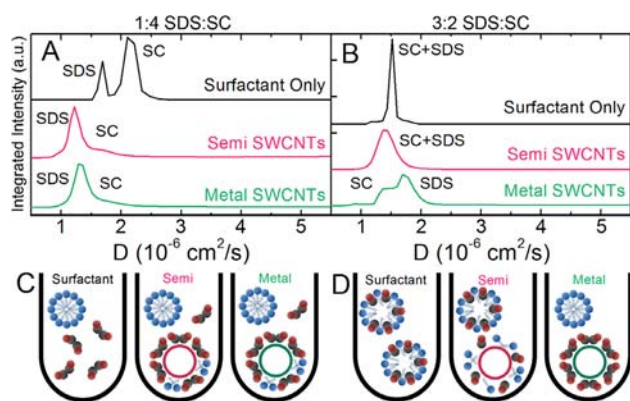


Figure 4. (Top) Integrated intensity versus D for surfactant only, semiconducting SWCNTs, and metallic SWCNTs in (A) 1:4 and (B) 3:2 SDS:SC. (Bottom) Representative cartoons of the surfactant only, semiconducting SWCNT, and metallic SWCNT micellar structures in (C) 1:4 and (D) 3:2 SDS:SC.

both SDS and SC exchange between the surfactant layers of the SWCNTs and the mixed micelle, and thus both molecules diffuse more slowly upon addition of SWCNTs. The metallic SWCNTs, however, segregate the mixed micelle: D for SDS in the 3:2 metallic SWCNT sample is the same as that for SDS in the 1:4 surfactant-only sample (Table S1), in which SDS forms a pure micelle, whereas D for SC is lower than those of the SC-only micelle and the mixed SDS/SC micelle. This result indicates that SC is the dominant surfactant for metallic SWCNTs, and the SDS in this sample is left to form pure micelles without SWCNTs. SC is predicted to form a well-packed monolayer on the SWCNT surface,⁸ while SDS forms an entropically favored disordered aggregate,¹⁸ so the co-surfactant micelle encapsulating the semiconducting SWCNTs in 3:2 will be less densely packed than the pure SC on the metallic SWCNTs, as indicated in the cartoon in Figure 4D.

The micellar structures deduced from the diffusion data led to the proposed explanation for DGU sorting of SWCNTs by electronic type. In general, a higher density of surfactant on the SWCNT surface will cause the SWCNT–surfactant complex to be more buoyant,¹⁹ but it is not the only determinant of buoyancy. As the SWCNT–surfactant system is a metastable colloidal dispersion, the balance between the attractive van der Waals (vdW) forces among SWCNTs and the Coulombic/steric repulsion between the ionic surfactants on the SWCNT surface will determine the degree of bundling (aggregation) of the nanotubes.²⁰ Larger bundles of SWCNTs are in general less buoyant than disaggregated SWCNTs, but previous quantitative analyses of single surfactant–SWCNT systems have shown that single SWCNT–surfactant complexes and small bundles containing a few SWCNTs can have the same buoyant density.⁸ Metallic SWCNTs have a larger polarizability, and thus larger vdW forces between them than semiconducting SWCNTs. In the case of the sample with a 1:4 mixture of surfactants (Figure 5A), the surfactant coverage on metallic and semiconducting SWCNT species is approximately equivalent, so we believe that the metallic SWCNTs are less buoyant because they form larger bundles, on average, than semiconducting SWCNTs, leading to a thin band of individualized (unbundled) semiconducting-enriched SWCNTs (red-orange) that is observed after DGU. We note that the small differences in surfactant coverage in 1:4 mixtures could be responsible for the subtle buoyant density

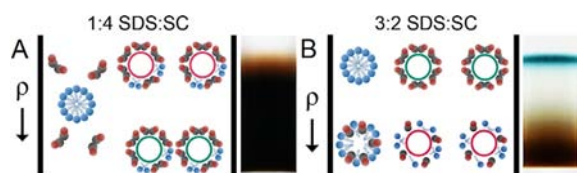


Figure 5. Depiction of semiconducting (pink) and metallic (green) SWCNTs in a density (ρ) gradient in surfactant ratios of (A) 1:4 and (B) 3:2 SDS:SC. The first column shows the local free-surfactant micellar structures, while the second shows two SWCNTs of a single electronic type and their micellar structure. Photographs of the centrifuge tubes show the position of semiconducting (red-orange) and metallic SWCNTs (green) after DGU.

differences, but this possibility appears unlikely since neither electronic type slows both surfactants more than the other.

In the sample of SWCNTs with a 3:2 mixture of surfactant, Figure 5B, the metallic SWCNTs (green) are encapsulated solely by SC, and the semiconducting SWCNTs (red-orange) are encapsulated by a two-surfactant micelle. The higher packing density of SC relative to an SDS/SC co-micelle results in a higher overall surface coverage, and thus a lower buoyant density, for metallic SWCNTs than semiconducting SWCNTs. Though the metallic SWCNTs have a higher polarizability and are thus more likely to bundle than semiconducting SWCNTs, SC is known to screen vdW forces better than SDS,²¹ so we suspect that the well-packed SC micelle inhibits this bundling and that the presence of SDS disrupts this screening in the 1:4 mixture. The stronger affinity of SC to metallic than semiconducting SWCNTs stems from stronger π - π interactions between metallic SWCNTs and the SC, as noted by previous literature.²²

In conclusion, we have utilized 2D DOSY NMR to probe the micellar structure of SDS and SC in aqueous solutions with and without addition of semiconducting and metallic SWCNTs. In the 1:4 mixture, the surfactant coverage of the metallic and semiconducting SWCNT species is very similar, so the larger density of the metallic SWCNTs is due to the larger polarizability of the metallic SWCNTs, which causes them to bundle more. In the 3:2 mixture, metallic SWCNTs interact selectively with SC while semiconducting SWCNTs interact with both surfactants, leading to large differences in surfactant coverage and thus in buoyant density. Future work to improve the purity of semiconducting and metallic SWCNTs separated by DGU could thus focus on studying the degree of bundling and increasing these differences by amplifying the vdW interactions in the 1:4 mixture and using different surfactant loadings in 3:2. Recent work by Tanaka et al. has demonstrated that other surfactants with straight alkyl tails and charged head groups can replace SDS in SWCNT separations and form similar micelles to SDS,²³ and our recent work has demonstrated the effects of surfactant loading on isolating high-purity diameter-sorted metallic SWCNTs.³ This work demonstrates the utility of 2D DOSY NMR in examining the interactions between SWCNTs and surfactants, which underlie the growing body of work on the fundamental science and applications of SWCNTs.²⁴

■ ASSOCIATED CONTENT

Supporting Information

Experimental details, peak identification and quantification, and calculation of micelle size. This material is available free of charge via the Internet at <http://pubs.acs.org>.

■ AUTHOR INFORMATION

Corresponding Author

m-hersam@northwestern.edu; e-weiss@northwestern.edu

Notes

The authors declare no competing financial interest.

■ ACKNOWLEDGMENTS

This material is based upon work supported by the National Science Foundation through a Graduate Research Fellowship (for A.J.M.-C. and T.A.S.) and through the Northwestern University Materials Research Science and Engineering Center (NU-MRSEC, NSF DMR-1121262).

■ REFERENCES

- (1) (a) Arnold, M. S.; Green, A. A.; Hulvat, J. F.; Stupp, S. I.; Hersam, M. C. *Nat. Nanotechnol.* **2006**, *1*, 60. (b) Liu, J.; Hersam, M. C. *MRS Bull.* **2010**, *35*, 315. (c) Hersam, M. C. *Nat. Nanotechnol.* **2008**, *3*, 387.
- (2) (a) Green, A. A.; Hersam, M. C. *Adv. Mater.* **2011**, *23*, 2185. (b) Ghosh, S.; Bachilo, S. M.; Weisman, R. B. *Nat. Nanotechnol.* **2010**, *5*, 443.
- (3) (a) Tyler, T. P.; Shastry, T. A.; Leever, B. J.; Hersam, M. C. *Adv. Mater.* **2012**, *24*, 4765. (b) Green, A. A.; Hersam, M. C. *Nano Lett.* **2008**, *8*, 1417.
- (4) Green, A. A.; Duch, M. C.; Hersam, M. C. *Nano Res.* **2009**, *2*, 69.
- (5) Cao, Q.; Rogers, J. A. *Adv. Mater.* **2009**, *21*, 29.
- (6) Avouris, P.; Chen, Z. H.; Perebeinos, V. *Nat. Nanotechnol.* **2007**, *2*, 605.
- (7) Carvalho, E. J. F.; dos Santos, M. C. *ACS Nano* **2010**, *4*, 765.
- (8) (a) Arnold, M. S.; Suntivich, J.; Stupp, S. I.; Hersam, M. C. *ACS Nano* **2008**, *2*, 2291. (b) Backes, C.; Karabudak, E.; Schmidt, C. D.; Hauke, F.; Hirsch, A.; Wohlleben, W. *Chem. Eur. J.* **2010**, *16*, 13176.
- (9) Moshhammer, K.; Hennrich, F.; Kappes, M. M. *Nano Res.* **2009**, *2*, 599.
- (10) (a) Hens, Z.; Moreels, I.; Martins, J. C. *ChemPhysChem* **2005**, *6*, 2578. (b) Fritzing, B.; Moreels, I.; Lommens, P.; Koole, R.; Hens, Z.; Martins, J. C. *J. Am. Chem. Soc.* **2009**, *131*, 3024.
- (11) (a) Chattopadhyay, D.; Galeska, I.; Papadimitrakopoulos, F. *J. Am. Chem. Soc.* **2003**, *125*, 3370. (b) Ju, S. Y.; Utz, M.; Papadimitrakopoulos, F. *J. Am. Chem. Soc.* **2009**, *131*, 6775. (c) Engtrakul, C.; Irurzun, V. M.; Gjersing, E. L.; Holt, J. M.; Larsen, B. A.; Resasco, D. E.; Blackburn, J. L. *J. Am. Chem. Soc.* **2012**, *134*, 4850.
- (12) Marega, R.; Aroulmoji, V.; Bergamin, M.; Feruglio, L.; Dinon, F.; Bianco, A.; Murano, E.; Prato, M. *ACS Nano* **2010**, *4*, 2051.
- (13) (a) Zhang, X. C.; Jackson, J. K.; Burt, H. M. *J. Biochem. Biophys. Methods* **1996**, *31*, 145. (b) Fuguet, E.; Ràfols, C.; Rosés, M.; Bosch, E. *Anal. Chim. Acta* **2005**, *548*, 95.
- (14) (a) Barnes, S.; Geckle, J. M. *J. Lipid Res.* **1982**, *23*, 161. (b) Stilbs, P. *J. Colloid Interface Sci.* **1982**, *87*, 385.
- (15) Wiedmer, S. K.; Riekkola, M. L. *Anal. Chem.* **1997**, *69*, 1577.
- (16) Tsybouski, D. A.; Bachilo, S. M.; Kolomeisky, A. B.; Weisman, R. B. *ACS Nano* **2008**, *2*, 1770.
- (17) Johnson, C. S., Jr. *J. Magn. Reson. A* **1993**, *102*, 214.
- (18) Tummala, N. R.; Striolo, A. *ACS Nano* **2009**, *3*, 595.
- (19) Nair, N.; Kim, W. J.; Braatz, R. D.; Strano, M. S. *Langmuir* **2008**, *24*, 1790.
- (20) Xu, Z.; Yang, X.; Yang, Z. *Nano Lett.* **2010**, *10*, 985.
- (21) Lin, S.; Blankschtein, D. *J. Phys. Chem. B* **2010**, *114*, 15616.
- (22) Lu, J.; Nagase, S.; Zhang, X.; Wang, D.; Ni, M.; Maeda, Y.; Wakahara, T. N.; Nakahodo, T.; Tsuchiya, T.; Akasaka, T.; Gao, Z.; Yu, D.; Ye, H.; Mei, W. N.; Zhou, Y. *J. Am. Chem. Soc.* **2006**, *128*, 5114.
- (23) Tanaka, T.; Urabe, Y.; Nishide, D.; Kataura, H. *J. Am. Chem. Soc.* **2011**, *133*, 17610.
- (24) Jariwala, D.; Sangwan, V. K.; Lauhon, L. J.; Marks, T. J.; Hersam, M. C. *Chem. Soc. Rev.* **2013**, DOI: 10.1039/c2cs35335k.